

Characterization of the Bose-glass phase in low-dimensional latticesJuan Carrasquilla,¹ Federico Becca,^{1,2} Andrea Trombettoni,^{1,3} and Michele Fabrizio^{1,2,4}¹*International School for Advanced Studies (SISSA), Via Beirut 2, I-34151 Trieste, Italy*²*Democritos Simulation Center, CNR-IOM Istituto Officina dei Materiali, Trieste, Italy*³*INFN, Sezione di Trieste, Trieste, Italy*⁴*International Centre for Theoretical Physics (ICTP), P.O. Box 586, I-34014 Trieste, Italy*

(Received 6 May 2010; published 27 May 2010)

We study by numerical simulation a disordered Bose-Hubbard model in low-dimensional lattices. We show that a proper characterization of the phase diagram on finite disordered clusters requires the knowledge of probability distributions of physical quantities rather than their averages. This holds in particular for determining the stability region of the Bose-glass phase, the compressible but not superfluid phase that exists whenever disorder is present. This result suggests that a similar statistical analysis should be performed also to interpret experiments on cold gases trapped in disordered lattices, limited as they are to finite sizes.

DOI: [10.1103/PhysRevB.81.195129](https://doi.org/10.1103/PhysRevB.81.195129)

PACS number(s): 05.30.Jp, 71.27.+a, 71.30.+h

I. INTRODUCTION

The impressive progresses in experiments with ultracold gases trapped in optical lattices have revived interest in old yet fundamental issues of many-body physics.¹ In fact, these systems give the unique opportunity to experimentally realize simple many-body models, such as the Bose or Fermi Hubbard models, which are believed to capture the essential physics underneath important phenomena, such as, for example, superfluidity or the Mott metal-insulator transition. Furthermore, most of the additional complications that arise in realistic materials can be avoided and the Hamiltonian parameters that identify these models are easily tunable in these experiments, unlike in realistic materials.

One of the first successes of these experiments has been the observation of a superfluid to Mott insulator transition in bosonic atoms trapped in optical lattices upon varying the relative strengths of interaction and interwell tunneling.² The possibility of introducing and tuning disorder, through speckles or additional incommensurate lattices, also led to the observation of Anderson localization for weakly interacting Bose gases.^{3,4} These important achievements progressively opened the way toward the challenging issue of realizing and studying a Bose-Hubbard model in the presence of disorder. Preliminary attempts to measure the excitation spectrum of interacting bosons in a disordered lattice⁵ have been performed by using Bragg spectroscopy.⁶

In spite of its simplicity, the disordered Bose-Hubbard model should allow one to “simulate” experimentally several interesting phenomena, such as, for example, the superconductor-to-insulator transition in thin films of dirty superconductors.^{7,8} We also mention that interacting bosonic models on a lattice are also relevant to describe magnetic systems in presence of a finite external magnetic field.⁹

The phase diagram of a disordered Bose-Hubbard model is supposed to include three different phases.^{10,11} When the interaction is strong and the number of bosons is a multiple of the number of sites, the model should describe a Mott insulator, with bosons localized in the potential wells of the optical lattice. This phase is neither superfluid nor compressible. When both interaction and disorder are weak, a super-

fluid and compressible phase must exist. These two phases are also typical of clean systems. In the presence of disorder, a third phase arises, the so-called Bose glass, which is compressible but not superfluid.¹¹ Indeed, when disorder is very strong, bosons localize in the deepest potential wells, which are randomly distributed. The coherent tunneling of a boson between these wells is suppressed just as in the usual Anderson localization, hence the absence of superfluidity, in spite of the fact that displacing a boson from one well to another one may cost no energy, hence a finite compressibility. Based on the same single-particle description used for explaining Anderson localization, it was argued that disorder prevents a direct superfluid-to-Mott insulator transition,¹¹ a speculation that has been subject to several theoretical studies.¹²⁻¹⁹

A simple way to justify the validity of the single-particle arguments is to imagine that the few carriers, which are released upon doping a Mott insulator, effectively behave as bosons at low density. In this case, the single-particle Anderson localization scenario is likely to be applicable since the few interacting bosons occupy strongly localized states in the Lifshitz tails. The implicit assumption is that the Mott-Hubbard side bands survive in the presence of disorder and develop Lifshitz’s tails that fill the Mott-Hubbard gap. This scenario is quite appealing hence worth to be investigated theoretically. However, a direct comparison of theory to experiments has to face the problem that experiments on cold gases are unavoidably limited to finite systems with hundreds of sites and finite number of disorder realizations. Therefore, objects such as Lifshitz’s tails, which arise from rare disorder configurations, might not be easily accessible. This fact demands an effort to identify salient features of the Bose glass that may distinguish the latter from a superfluid or a Mott insulator already on finite systems.

This is actually the scope of this work. Specifically, we are going to show that the statistical distribution of the energy gaps extracted by a numerical simulation of finite-size systems is a significant property that can discriminate among different phases. The numerical simulations have been carried out for a single chain, a two- and three-leg ladder system, and finally for a genuine two-dimensional lattice. The ladder systems are of interest because they can be experimentally realized not only in optical lattices but also in mag-

netic materials. Indeed, very recent neutron-scattering data reported the evidence of the spin—analogue of a Bose—glass phase in a spin-ladder compound in which disorder was induced by random chemical substitution.²⁰ Finally, we shall also discuss how the probability distribution of the energy gaps could be experimentally accessed.

The paper is organized as follows. In Sec. II, we present the model and briefly discuss our numerical methods. In Sec. III, we present and discuss our results. Finally, Sec. IV is devoted to concluding remarks.

II. MODEL AND METHOD

The simplest Hamiltonian that contains the basic ingredients of strong correlations and disorder is the Bose-Hubbard model

$$\mathcal{H} = -\frac{t}{2} \sum_{\langle i,j \rangle} b_i^\dagger b_j + \text{H.c.} + \sum_i \left(\frac{U}{2} n_i(n_i - 1) + \epsilon_i n_i \right), \quad (1)$$

where $\langle \dots \rangle$ indicates nearest-neighbor sites, b_i^\dagger (b_i) creates (annihilates) a boson on site i , and $n_i = b_i^\dagger b_i$ is the local-density operator. The on-site interaction is parametrized by U , whereas the local disordered potential is described by random variables ϵ_i that are uniformly distributed in $[-\Delta, \Delta]$. Here, we consider bosons on a one-dimensional (1D) chain, N -leg ladders, and a two-dimensional (2D) square lattice.

We study model (1) by Green's function Monte Carlo with a fixed number M of bosons on L sites,²¹ $n = M/L$ being the average density. We recall that this is a zero-temperature algorithm that provides numerically exact results because of the absence of sign problem. One starts from a trial (e.g., variational) wave function and filters out high-energy components by iterative applications of the imaginary-time evolution operator. In order to improve the numerical efficiency, it is important to consider an accurate starting wave function. In the clean case, we have recently shown²² that good accuracy can be achieved by applying a density-density Jastrow factor to a state where all bosons are condensed at $q=0$, i.e.,

$$|\Psi_{\text{clean}}\rangle = \exp \left\{ -\frac{1}{2} \sum_{ij} v_{i,j} (n_i - n)(n_j - n) \right\} |\Phi_0\rangle, \quad (2)$$

where $|\Phi_0\rangle = (\sum_i b_i^\dagger)^M |0\rangle$ is the noninteracting Bose condensate of M particles, $(n_i - n)$ is the variation of the on-site density with respect to the average value n , and $v_{i,j}$ are translationally invariant parameters that are determined by minimizing the variational energy.²³

In the presence of disorder, we just add to Eq. (2) a *site-dependent* one-body Jastrow factor

$$|\Psi\rangle = \exp \left\{ \sum_i g_i n_i \right\} |\Psi_{\text{clean}}\rangle, \quad (3)$$

where g_i 's are L additional variational parameters. This wave function becomes the exact ground state for $U=0$ and finite Δ if $v_{i,j}=0$ and $g_i = \ln \alpha_i$, with α_i being the amplitude at site i of the lowest-energy single-particle eigenstate of the noninteracting Hamiltonian. A similar wave function has been

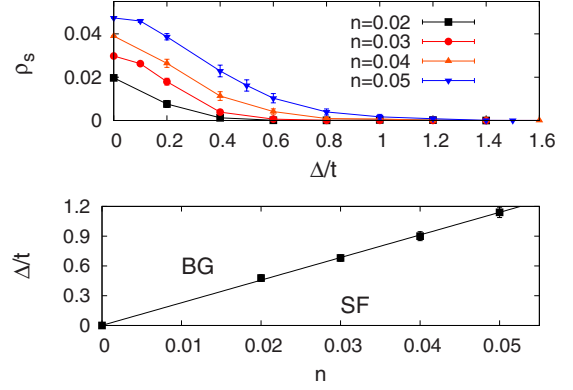


FIG. 1. (Color online) Upper panel: superfluid stiffness ρ_s as a function of the disorder strength Δ/t for different densities of hard-core bosons. Lower panel: low-density phase diagram of the hard-core bosonic model. Calculations have been done on a 2×50 ladder system.

recently used to describe the fermionic Hubbard model in the presence of disorder.²⁴ The flexibility of this variational state makes it possible to describe equally well superfluid, Bose-glass, and Mott insulating states.

We conclude this section by mentioning that, in a realistic experimental setup, a two-leg ladder may be realized by combining a double-well potential along a direction (say, x) and two potentials along the z axis, one of them creating a cigar geometry and the other one to create the periodic lattice. By using a double-well potential such as in Ref. 25, with a distance $\sim 5 \mu\text{m}$ and a barrier $\sim h \times 500$ Hz between sites of different legs, one gets for a number of particles $M \sim 100$ an interleg tunneling rate $t_\perp \sim h \times 5$ Hz. Moreover, with a distance $\sim 0.5 \mu\text{m}$ and a barrier $\sim h \times 10$ KHz between sites in the same leg, one gets an intraleg tunneling rate $t_\parallel \sim t_\perp$. Therefore, it is not unrealistic to consider a space-isotropic hopping, equal along all bonds, which we will assume hereafter.

III. RESULTS

In this section, we present our numerical results for the Bose-Hubbard model (1). First, we briefly discuss the case of hard-core bosons (i.e., $U=\infty$) at low densities on a two-leg ladder. Then we consider the case of soft-core bosons at filling one, i.e., $n=1$, which represents the main subject of this work.

A. Hard-core bosons at low densities

Figure 1 shows the low-density phase diagram of hard-core bosons on a two-leg ladder. We find that for any finite disorder Δ , the low-density phase is a Bose glass that turns superfluid above a critical density. In other words, the trivial Mott insulator with no bosons is indeed separated from the superfluid phase by a Bose glass. We emphasize that the existence of a superfluid phase for hard-core bosons in a two-leg ladder is *per se* remarkable. Indeed, in a single chain with nearest-neighbor hopping, hard-core bosons are equivalent to spinless fermions, which Anderson localized for any

density and in any dimension $D \leq 2$. Consequently, hard-core bosons on a single chain are never superfluid. Already in a two-leg ladder, hard-core bosons start to behave differently from spinless fermions. Indeed, while the latter ones remain always localized, the former ones show a superfluid phase. We just mention that the same occurs also on a single chain with longer-range hopping.

B. Soft-core bosons at $n=1$

We now turn to finite on-site interactions and consider the case with $n=1$. The Bose-Hubbard model has been extensively studied in recent years,^{12–19} with special focus on the question whether a direct superfluid to Mott insulator transition does exist or not. This issue has been finally solved only recently. The solution is based on the observation that, if the disorder strength Δ is larger than half of the energy gap of the clean Mott insulator E_g^{clean} , then the ground state must be compressible, otherwise is incompressible.^{18,26} Therefore, the independent measurements of the superfluid stiffness ρ_s at finite Δ and of the clean Mott gap E_g^{clean} allow a precise determination of the phase boundaries between different phases and demonstrate unambiguously the existence of a Bose glass in between the superfluid and Mott phases.^{18,19} The above prescription is very effective in a numerical simulation since both ρ_s with disorder and E_g^{clean} without disorder can be determined quite accurately. In a real experiment, such a prescription is difficult to put in practice as it requires the knowledge of E_g^{clean} and an estimate of the disorder strength. Instead, it would be more desirable to have a simple criterion to establish directly the nature of the phase of a given system in a realistic finite-size experimental setup. In a clean system, this program can be accomplished by measuring the gap, conventionally defined by $E_g = \mu^+ - \mu^-$, where $\mu^+ = E_{M+1} - E_M$ and $\mu^- = E_M - E_{M-1}$ (E_M being the ground-state energy with M particles). Experimental estimates for the gap have been so far obtained in ultracold atomic systems mainly in two ways: one consists in applying a gradient potential that compensates the Mott energy gap and allows tunneling between neighboring sites;² the other method exploits a sinusoidal modulation of the main lattice height for stimulating resonant production of excitations.^{5,6}

In disordered systems, the Mott gap can be overcome by transferring particles between two regions with almost flat disorder shifting the local chemical potential upward and downward, respectively. These regions may be far apart in space and represent rare fluctuations (Lifshitz's tail regions). Therefore, it is quite likely that the conventional definition of the gap

$$\bar{E}_g = \frac{1}{\mathcal{N}} \sum_{\alpha=1, \dots, \mathcal{N}} (\mu_{\alpha}^+ - \mu_{\alpha}^-), \quad (4)$$

where α denote the disorder realizations, will miss the Lifshitz's tails for any accessible number of disorder realizations \mathcal{N} . This fact could give a finite gap even when the actual infinite system would be compressible. To circumvent such a difficulty, it is useful to imagine that a large systems is made by several subsystems, each represented by the L -site cluster under investigation, and construct the gap by using

μ^+ and μ^- from *different* disorder realizations. In other words, one could define an alternative estimate of the gap as

$$E_g^{\text{min}} = \min_{\alpha, \beta} |\mu_{\alpha}^+ - \mu_{\beta}^-|, \quad (5)$$

with all the disorder realizations α and β . In the limit of very large systems where boundary effects become negligible, E_g^{min} must eventually coincide with \bar{E}_g . In finite systems, the two estimates differ, nevertheless we believe that E_g^{min} is more representative than the average value. Besides E_g^{min} , one can define the full gap distribution

$$P(E_g) = \sum_{\alpha, \beta} \delta(E_g - \mu_{\alpha}^+ + \mu_{\beta}^-), \quad (6)$$

which we will show has remarkable properties. We mention that, by our definition, $P(E_g < 0)$ could well be finite on finite systems, although it must vanish in the thermodynamic limit where $P(E_g)$ becomes peaked at a single positive (or vanishing) value, i.e., the actual gap. In experiments with ultracold atoms, both E_g^{min} and $P(E_g)$ could be accessed by measuring *separately* μ^+ and μ^- for different disorder realizations. For instance, one could measure the energy releases E_M^{rel} of falling atoms when the trap is turned off with the reference number of particles M and with numbers $M \pm M'$. For $M' \ll M$, indeed $E_{M+M'}^{\text{rel}} - E_M^{\text{rel}} \simeq M' \mu^+$ and $E_M^{\text{rel}} - E_{M-M'}^{\text{rel}} \simeq M' \mu^-$.

Let us start from the 1D case, whose zero-temperature phase diagram has been worked out by density-matrix renormalization group (DMRG).²⁷ At finite values of Δ , the on-site interaction U turns the Bose glass into a superfluid, which remains stable up to $U = U_{c1}$, where ρ_s vanishes. However, the system remains gapless for $U_{c1} < U < U_{c2}$, indicating the presence of a Bose-glass phase. At $U = U_{c2}$, the system turns into an incompressible Mott insulator. For $\Delta/t = 2$, we have that $U_{c1}/t \simeq 3.7$. If we use \bar{E}_g as estimator of the actual gap, we find that the Bose glass survives up to $U_{c2}/t \simeq 5$, not far from the DMRG estimate,²⁷ but smaller than the value predicted by the condition $\Delta = E_g^{\text{clean}}/2$, which would lead to $U_{c2}/t \simeq 6.9$. As discussed before, this discrepancy arises by the inability to catch rare disorder configurations, which could be overcome by analyzing the minimum gap E_g^{min} and the full distribution probability $P(E_g)$. Indeed, when using E_g^{min} as a detector of gapless excitations, we obtain an estimate of $U_{c2}/t \simeq 6.2$, much closer to the expected value $U_{c2}/t \simeq 6.9$. As far as $P(E_g)$ is concerned, we note that it behaves quite differently in the three different phases (see Fig. 2). As long as the phase is superfluid, $P(E_g)$ is peaked at $E_g = 0$. In the Bose glass, $P(E_g)$ is instead peaked at a finite $E_g > 0$, yet $P(0)$ stays finite. In the Mott insulator, $P(E_g)$ remains peaked at a positive E_g but $P(0) = 0$. This suggests that $P(E_g)$ could also be an efficient tool for discriminating between different phases.

Let us now analyze the evolution of the phase diagram when the 2D limit is approached by increasing the number of legs. Moving from $D=1$ to $D=2$, the stability region of the Bose glass is expected to shrink,¹¹ making its observation in experiments more and more difficult. In Fig. 3, we show our results for two- and three-leg ladders and, for comparison, also the 2D limit (evaluated for a rather small 12×12 cluster). In this case, we take $\Delta/t = 5$, in order to have a larger

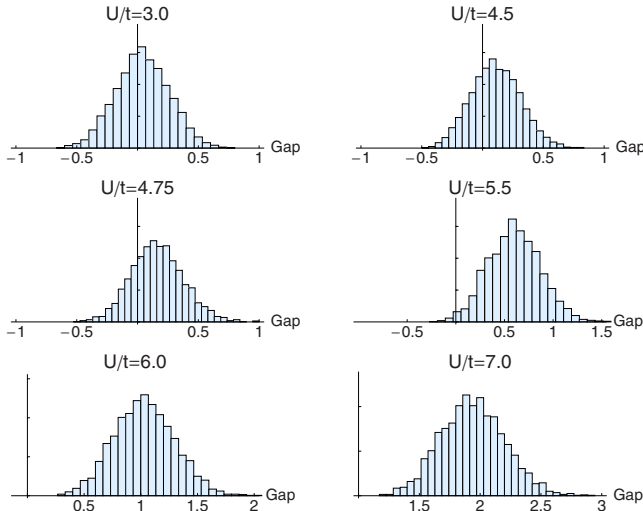


FIG. 2. (Color online) Distribution $P(E_g)$ of the gap in the 1D Bose-Hubbard model for different values of U/t and $L=60$ sites.

Bose-glass region in between the superfluid and the Mott phases. In 1D, for such large disorder strength, no superfluidity is found at all. By increasing the number of legs, we rapidly converge to the 2D results: this fact is particularly clear from the data on the gap. Both the results on the minimum gap and the ones that come from $\Delta = E_g^{\text{clean}}/2$ show that the critical U for the Mott transition is almost the same for three legs and 2D. Also, the superfluid stiffness ρ_s seems to rapidly converge from below to the 2D limit. We also find that the behavior of $P(E_g)$ is qualitatively similar to what found in 1D, confirming that it can actually discriminate among the different phases (see Fig. 4). We mention that, should we use as estimator of the gap \bar{E}_g , we would have concluded that the Bose glass never exists in 2D and that a direct superfluid to Mott insulator transition occurs. The use of E_g^{min} instead demonstrates that the Bose glass does exist also in 2D and always intrudes between the superfluid and the Mott insulator.

In Fig. 5, we plot the density profile for a given disorder configuration on the 2×40 ladder. As soon as the on-site interaction is finite, particles become rather delocalized and

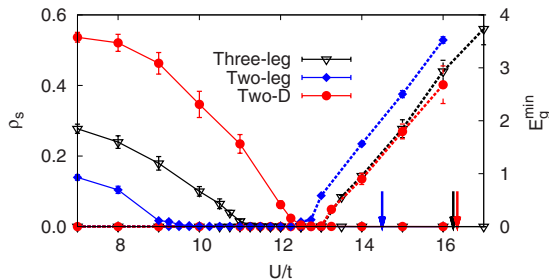


FIG. 3. (Color online) Superfluid stiffness ρ_s (solid lines on the left) and the minimum gap E_g^{min} (dashed lines on the right) for different clusters. Two-leg (with 2×40 sites) and three-leg (with 3×50) ladders are shown; the 2D case with a 12×12 cluster is also reported for comparison. In all cases, the disorder strength is $\Delta/t = 5$. Arrows indicate the opening of the charge gap according to $\Delta = E_g^{\text{clean}}/2$.

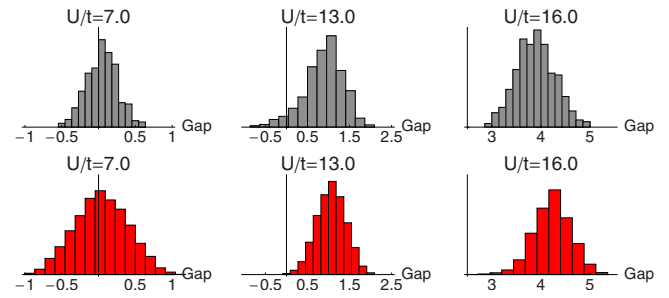


FIG. 4. (Color online) Distribution $P(E_g)$ of the gap for the three-leg ladder 3×50 (upper row) and 2D 12×12 (lower row) for different values of U/t . In all cases, the disorder strength is $\Delta/t = 5$.

many sites of the lattice acquire a finite-boson density. There are large fluctuations in the local density with n_i ranging from ≈ 0 to $n_i^{\text{max}} \approx 4$. Although there is a number of sites with very small density, the superfluid stiffness is finite [e.g., $\rho_s = 0.015(2)$ for $U/t = 1$]. We notice that, in spite of the disorder being uncorrelated from site to site, there is a strong density correlation between the two legs. By increasing further U/t , the density becomes more and more homogeneous (for $U/t = 5$, $n_i^{\text{max}} \approx 2$, still with rather large fluctuations). ρ_s has a maximum $U/t \approx 5$ and then is suppressed [e.g., $\rho_s = 0.0015(5)$ at $U/t = 11$]. However, as far as the local density is concerned, we do not observe a drastic modification between the superfluid (e.g., $U/t \lesssim 9$) and the Bose glass (e.g., $U/t \gtrsim 9$), even though fluctuations look considerably suppressed for $U/t = 11$ (see Fig. 5). Eventually, for $U/t \geq 12$, the incompressible Mott phase is reached, with very small density fluctuations ($n_i \approx 1$), which are not very different from the ones observed in the Bose glass close to the transition.

We finish by showing variational results for the momentum distribution $n_k = \langle b_k^\dagger b_k \rangle$ for the same ladder system. In Fig. 6, we show the results for different values of U/t (we also report the results for the variational gap). Since, this is an almost 1D system, no condensation fraction is found (i.e., $n_0/L \rightarrow 0$ in the thermodynamic limit). However, the super-

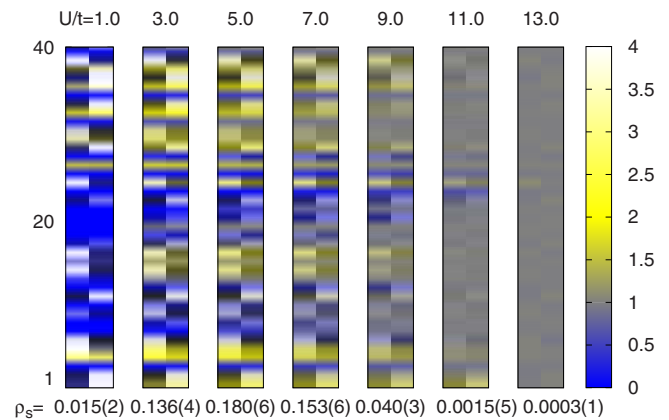


FIG. 5. (Color online) Local density for one disorder realization of the 2×40 ladder. Darker (brighter) spots indicate lower (higher) densities. The values of the stiffness ρ_s for the same disorder realization are also reported.

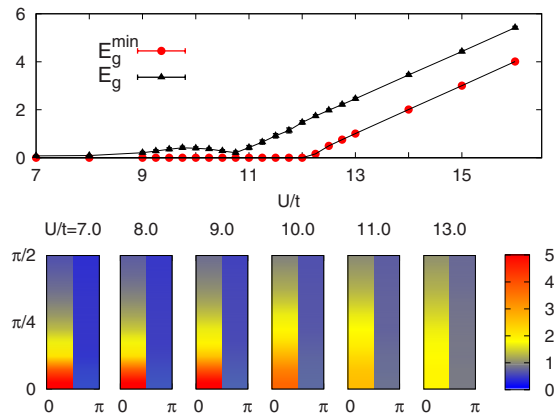


FIG. 6. (Color online) Upper panel: variational results for the excitation gap for a 2×40 ladder. Lower panels: momentum distribution n_k for the same cluster.

fluid phase is characterized by quasi-long-range order with a cusp in n_k and a logarithmic divergent n_0 . On the other hand, both the Bose-glass and the Mott phases have a smooth momentum distribution, with $n_0 \rightarrow \text{const}$ in the thermodynamic limit.

IV. CONCLUSIONS

We have presented a detailed study of the ground-state properties of the disordered Bose-Hubbard model in low-

dimensional lattices, relevant for on-going experiments with cold atomic gases trapped in optical lattices. We have determined the distribution probability of the gap on finite sizes and shown that it contains useful information. In particular, we have found that the Bose glass is characterized by a broad distribution of the gap that is peaked at finite energy but extends down to zero, a shape remarkably reminiscent of preformed Hubbard sidebands with the Mott gap completely filled by Lifshitz's tails. The Mott transition occurs when these tails terminate at finite energy. On the contrary, the gap distribution in the superfluid phase turns out to be strongly peaked at zero energy. These results suggest a simple and efficient way to discriminate between different phases in experiments, which, being performed on finite systems, suffer from the same size limitations as our simulations.

We have also investigated the disordered Bose-Hubbard model on N -leg ladder systems, emphasizing that these geometries could be quite useful to study the evolution from one to two spatial dimensions. Experiments with both cold atomic gases and magnetic systems are becoming now possible on ladders, hence we believe that our calculations may represent an important benchmark in this direction.

ACKNOWLEDGMENTS

We thank C. Castellani, L. Fallani, and C. Fort for useful discussions. Calculations have been performed on the cluster Matrix of CASPUR, thanks to Standard HPC Grant 2009.

- ¹I. Bloch, J. Dalibard, and W. Zwerger, *Rev. Mod. Phys.* **80**, 885 (2008).
- ²M. Greiner, O. Mandel, T. Esslinger, T. E. Hansch, and I. Bloch, *Nature (London)* **415**, 39 (2002).
- ³J. Billy, V. Josse, Z. Zuo, A. Bernard, B. Hambrecht, P. Lugan, D. Clement, L. Sanchez-Palencia, P. Bouyer, and A. Aspect, *Nature (London)* **453**, 891 (2008).
- ⁴G. Roati, C. D'Errico, L. Fallani, M. Fattori, C. Fort, M. Zaccanti, G. Modugno, M. Modugno, and M. Inguscio, *Nature (London)* **453**, 895 (2008).
- ⁵L. Fallani, J. E. Lye, V. Guarrera, C. Fort, and M. Inguscio, *Phys. Rev. Lett.* **98**, 130404 (2007).
- ⁶T. Stöferle, H. Moritz, C. Schori, M. Köhl, and T. Esslinger, *Phys. Rev. Lett.* **92**, 130403 (2004).
- ⁷M. Ma, B. I. Halperin, and P. A. Lee, *Phys. Rev. B* **34**, 3136 (1986).
- ⁸M. P. A. Fisher, *Phys. Rev. Lett.* **65**, 923 (1990).
- ⁹T. Giamarchi, C. Rugg, and O. Tchernyshev, *Nat. Phys.* **4**, 198 (2008).
- ¹⁰T. Giamarchi and H. J. Schulz, *Europhys. Lett.* **3**, 1287 (1987); *Phys. Rev. B* **37**, 325 (1988).
- ¹¹M. P. A. Fisher, P. B. Weichman, G. Grinstein, and D. S. Fisher, *Phys. Rev. B* **40**, 546 (1989).
- ¹²J. K. Freericks and H. Monien, *Phys. Rev. B* **53**, 2691 (1996).
- ¹³R. T. Scalettar, G. G. Batrouni, and G. T. Zimanyi, *Phys. Rev. Lett.* **66**, 3144 (1991).
- ¹⁴W. Krauth, N. Trivedi, and D. Ceperley, *Phys. Rev. Lett.* **67**, 2307 (1991).
- ¹⁵R. V. Pai, R. Pandit, H. R. Krishnamurthy, and S. Ramasesha, *Phys. Rev. Lett.* **76**, 2937 (1996).
- ¹⁶J.-W. Lee, M.-C. Cha, and D. Kim, *Phys. Rev. Lett.* **87**, 247006 (2001).
- ¹⁷N. Prokof'ev and B. Svistunov, *Phys. Rev. Lett.* **92**, 015703 (2004).
- ¹⁸L. Pollet, N. V. Prokofev, B. V. Svistunov, and M. Troyer, *Phys. Rev. Lett.* **103**, 140402 (2009).
- ¹⁹V. Gurarie, L. Pollet, N. V. Prokofev, B. V. Svistunov, and M. Troyer, *Phys. Rev. B* **80**, 214519 (2009).
- ²⁰T. Hong, A. Zheludev, H. Manaka, and L.-P. Regnault, *Phys. Rev. B* **81**, 060410(R) (2010).
- ²¹M. Calandra Buonaura and S. Sorella, *Phys. Rev. B* **57**, 11446 (1998).
- ²²M. Capello, F. Becca, M. Fabrizio, and S. Sorella, *Phys. Rev. Lett.* **99**, 056402 (2007); *Phys. Rev. B* **77**, 144517 (2008).
- ²³S. Sorella, *Phys. Rev. B* **71**, 241103(R) (2005).
- ²⁴M. E. Pezzoli, F. Becca, M. Fabrizio, and G. Santoro, *Phys. Rev. B* **79**, 033111 (2009); M. E. Pezzoli and F. Becca, *ibid.* **81**, 075106 (2010).
- ²⁵M. Albiez, R. Gati, J. Folling, S. Hunsmann, M. Cristiani, and M. K. Oberthaler, *Phys. Rev. Lett.* **95**, 010402 (2005).
- ²⁶P. B. Weichman, *Mod. Phys. Lett. B* **22**, 2623 (2008).
- ²⁷S. Rapsch, U. Schollwock, and W. Zwerger, *EPL* **46**, 559 (1999).